JOURNAL OF MATERIALS SCIENCE 27 (1992) 1440–1444

Effect of melt temperature on the formation of air pockets during splat quenching

WEN-KUAN WANG, CHENG-TZU KUO
Institute of Mechanical Engineering, National Chiao Tung University, Hsinchu, 30050, Taiwan
TSUNG-SHUNE CHIN
Department of Materials Science and Engineering, National Tsing Hua University, Hsinchu, 30043, Taiwan

The effect of melt temperature on the formation of air pockets at the contact surface of the ribbons was studied. An alloy with a melting point slightly higher than room temperature (320 K) was used and was heated to 353, 573 and 773 K, respectively, to investigate the thermal effect of the melt temperature on the gas. Under high casting velocity (20 $m s^{-1}$) and extremely low melting temperature (353 K), the air pockets were slender and parallel to the casting direction. The liquid melts with a higher casting temperature (773 K) induced coarse air pockets at various casting velocities, and the air pockets were coarser than those induced by the pressure of the gas boundary layer only. The heat flow analysis showed that the local pressure of the entrapped gas, built up by the thermal effect and assuming constant volume, is far greater than the pressure by the gas-boundary layer effect. Thus the thermal effect of the liquid melt should be taken into account in the formation of air pockets during splat quenching.

1. Introduction

In the last two decades much attention has been paid to the manufacture of rapidly solidified ribbons from the melt by the single-roller quenching method, because of the simplicity in facilities and effectiveness in producing amorphous or microcrystalline alloys [1–4]. During casting, the melt in the liquid puddle is dragged away by the high-speed rotating substrate, resulting in a converging contact angle between the upstream free surface of the puddle and the substrate. The converging contact angle is suffered by the impacting of the gas-boundary layer on the wheel surface associated with the rotating wheel. A noncontact area on the contact surface of the cast ribbon is thus formed [5, 6] and results in a poor ribbon quality [7, 8]. Except for the above gas-boundary effect, the negative pressure region present at the rear of the liquid puddle [9], or the ability of the melts to conform to the microtopography of the substrate, were also proposed as possible mechanisms of air pocket formation [10].

The formation of an air pocket is a phenomenon where the melt in the puddle is lifted from the wheel surface, about several micrometres in height, by the pressure of the gas during casting. The lifting force applied by the gas in the converging contact angle includes the accumulation of the pressure of the gas-boundary layer [5, 6] and thermal expansion of the gas. The gas on the wheel surface associated with the rotating wheel is originally at about room temperature. As soon as the gas intimately contacts the high-temperature melt, it will rapidly be heated and develop a local high-pressure region. The temperature difference between the melt and the gas may reach several hundreds or even one thousand or more degrees Kelvin, depending on the temperature of the melt. However, the role of the thermal effect of the gas on promoting the air pocket formation has not been taken into consideration before.

In this work, the possibility of enhancing air pocket formation by the thermal effect of the melt temperature on the gas was elucidated. An alloy with a melting temperature slightly higher than room temperature (320 K) was used and was heated to 353, 573 and 773 K, to determine the effect of melt temperature on air pocket formation during casting. The rate and the value of pressure built up by the thermal effect of the melt on the entrapped gas were calculated by a heat flow analysis, and compared with the pressure built up by the gas-boundary layer effect.

2. Experimental procedure

A low melting point alloy, nominal composition $Bi_{44.7}Pb_{22.6}Sn_{8.3}Cd_{5.3}In_{19.1}$ (melting point 320 K), was used as the casting material, and the casting temperature was carefully fixed at 353, 573, and 773 K. A circular orifice was provided at the bottom of the crucible, and the height of falling distance of the droplets was fixed at 50 mm. The weight of the liquid drops was about 0.04 g in this study. The substrate was a stainless steel wheel rotating at substrate speeds of 5–20 $m s^{-1}$. Prior to each run, the substrate was polished by a grit 800 abrasive paper. As the liquid drops fell on to the rotating substrate, the melt was

0022–2461

dragged away by the substrate, and a thin solidified ribbon was formed. Owing to good wetting of this liquid melt on the substrate, the spun ribbons always stuck to the rotating substrate, and could not be flung away from the substrate by the centrifugal force.

3. Results and discussion

3.1. Contact patterns of the solidified ribbons

Splat quenching a liquid drop onto a rotating substrate is a complicated form of the rapid solidification process. This is due to the complex heat-transfer behaviour between the melt and the substrate, and the complex internal fluid flow field of the liquid melt as the melt spreads following the droplet impact on the substrate. At the initial stage, the kinetic energy of the drop, as it strikes the substrate, will produce a contact pressure between the melt and the substrate. At a later stage, the kinetic energy is lost due to spreading of the melt and resting on the substrate. As a result, the contact pattern of the solidified ribbon is always better in the initial stage than in the later stage, i.e. the puddle stability is time-dependent during casting. A typical solidified ribbon is shown in Fig. 1. In this study, in order to compare the contact patterns with different casting temperatures under the same puddle stability, the contact patterns of the solidified ribbons were taken and compared at a fixed position 10 mm from the initial end of the ribbon.

The contact patterns of the cast ribbons are shown in Fig. 2. Comparing Fig. 2a, b and c, for casting temperatures of 353, 573 and 773 K, respectively (same casting velocity of 5 $m s^{-1}$), it is interesting to note that the melt temperature plays a significant role on the air pocket formation. At a lower melt temperature, e.g. 353 K, no air pocket is formed, due to either the pressure of the gas-boundary layer or the thermal effect of the melt temperature on the gas. However, as the melt temperature increases to 573 K, air pockets form parallel to the casting direction. As the melt temperature reaches 773 K, the size of the air pockets is coarser than those cast at 573 K. The driving force of this air pocket formation is believed to be the thermal effect of the melt temperature on the gas. On increasing the casting velocity to 10 $m s^{-1}$, the size and number of air pockets are similar to those at a casting velocity of 5 $m s^{-1}$, as shown in Fig. 2d, e and f for casting temperatures of 353, 573 and 773 K, respectively (same casting velocity of 10 $m s^{-1}$). This experiment shows that the effect of the melt temperature on air pocket formation does not necessarily occur at relatively high temperatures (e.g. above 1000 K), and the size and morphology of air pockets is sensitive to the melt temperature. The above results also show that the thermal effect can not only enlarge the air pockets, but can also induce the formation of air pockets.

At a casting temperature of 353 K and low casting velocity (less than 15 $m s^{-1}$), no air pockets are formed due to the gas-boundary layer effect. Up to a casting velocity of > 17.5 $m s^{-1}$, air pockets are formed, as shown in Fig. 3. The size of the air pockets formed under these conditions is small and parallel to the casting direction. Increasing the casting velocity will increase the rate of dragging the melt away from the puddle by the rotating substrate, and may result in a smaller contact angle. At the same time, the upstream free surface of the liquid puddle, which freely stands on the rotating substrate, is disturbed by the larger pressure of the gas-boundary layer, suggesting that the puddle stability is poorer. Thus, the gas in the interface between the puddle and the substrate is more readily entrapped by the puddle under these high casting velocity condition. However, comparing Figs 3 and 2c, it is clear that the air pockets induced by the thermal effect (melt temperature 773 K) are still much coarser than those induced by the gas-boundary layer effect only. The difference in the morphology and size of air pockets between Figs 3 and 2c is believed to arise from the different driving forces of air pocket formation.

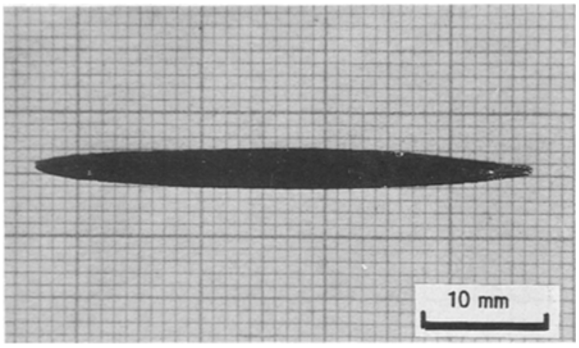

Figure 1 A solidified ribbon after the impingement of a falling-droplet on a rotating substrate; casting direction from right to left.

3.2. Local pressure increase rate of the entrapped gas by the thermal effect

The gas on the wheel surface is originally at about room temperature. If the gas is intimately in contact with the melt, it will then be heated and develop a local high-pressure region. The converging contact angle between the melt and the substrate is dynamic and complex. At the instant of air pocket formation, part of the gas in the gas-boundary layer will penetrate into the liquid puddle and part will be retarded by the free surface of the puddle. On the other hand, if the contact between the melt and the substrate is stable (or the contact angle is large), all the gas in the boundary layer will be retarded. In order to calculate the temperature and pressure increase rate of the entrapped gas in such a dynamic condition, a simplified geometry for the gas between the melt and the substrate, as shown in Fig. 4, is used to simulate the thermal effect of the melt on the gas, and the following assumptions are made.

1. The heat transfer from the melt to the gas is through conduction only. We neglect the contribution of convection and radiation.

2. The initial conditions of the entrapped gas are assumed to be at room temperature and 1 atm pressure.

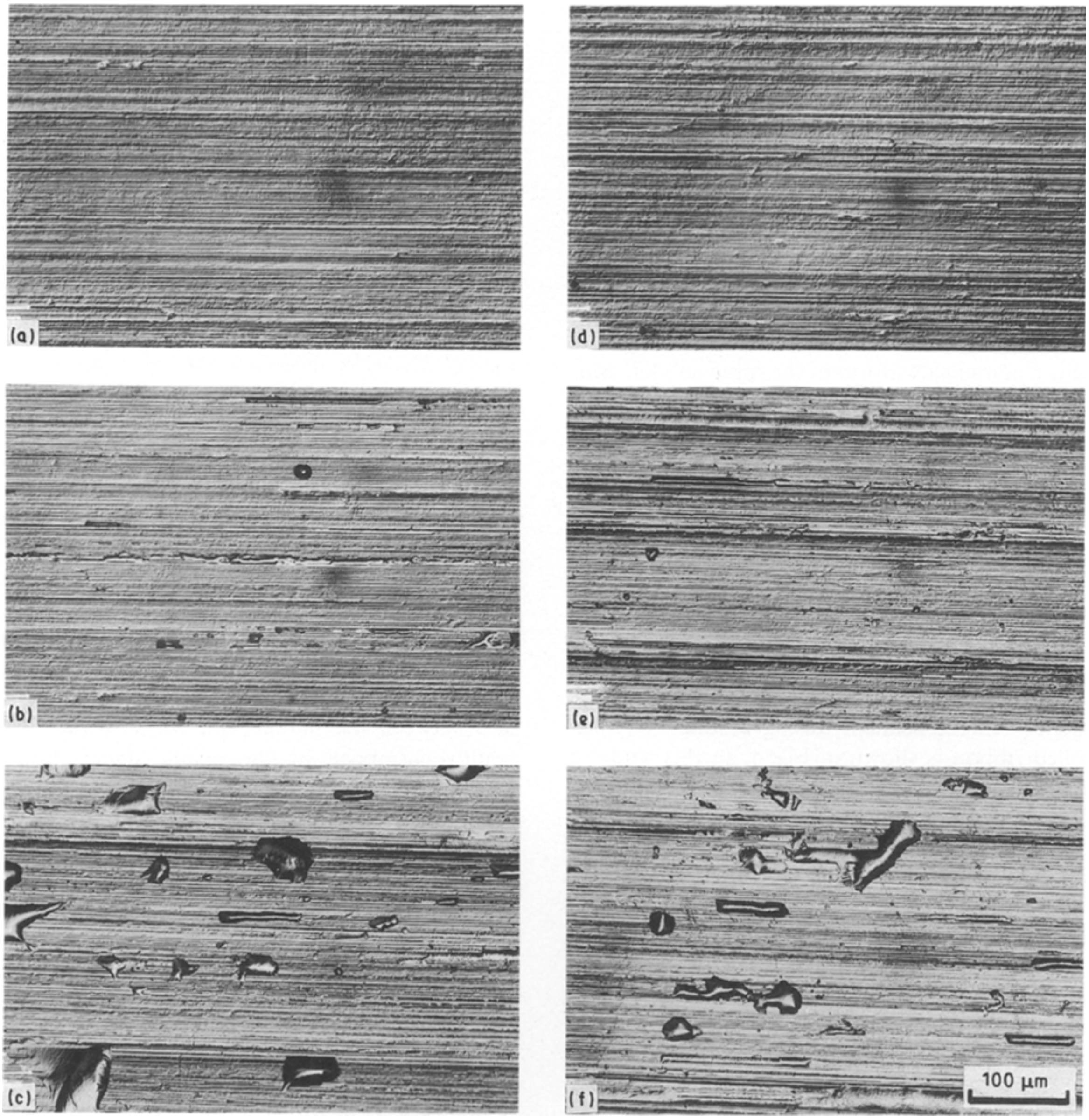

Figure 2 The contact patterns of the solidified ribbons: (a–c) at a casting velocity of $5\ \mathrm{m\,s^{-1}}$ and casting temperature of 353, 573 and 773 K, respectively; (d–f) at a casting velocity of $10\ \mathrm{m\,s^{-1}}$, and casting temperature of 353, 575 and 773 K, respectively.

3. The temperatures of the melt and the substrate are assumed to remain constant during the short gas-expansion period (of the order of a microsecond).

The gas temperature can be determined by solving the differential equation for heat flow, assuming constant thermal properties of the gas

$$\frac{\partial T}{\partial t} = \alpha \frac{\partial^2 T}{\partial^2 y} \quad (1)$$

where T is the temperature, t the time, and α the thermal diffusivity of air, which is assumed to be constant, $3.0 \times 10^{-5}\ \mathrm{m^2\,s^{-1}}$. The gas temperature distribution is then obtained as

$$T(y, t) = T_1 + \frac{(T_2 - T_1)}{l} y + \frac{2(T_1 - T_2)}{\pi} \sum_{n=1}^{\infty} \frac{(-1)^{n+1}}{n} \sin\frac{n\pi y}{l} \exp\left[-\left(\frac{n\pi}{l}\right)^2 \alpha t \right] \quad (2)$$

where T_1 is the substrate temperature and the initial gas temperature, T_2 the melt temperature, and l the depth of the entrapped gas, as shown in Fig. 4. Then, the mean temperature of the gas is given by

$$T_{\mathrm{m}} = \frac{1}{l} \int_0^l T(y, t) \mathrm{d}y \quad (3)$$

The lifting of the melt off the wheel surface is driven by pressure of the entrapped gas. In order to calculate the amount of pressure built up from the contribution of the thermal effect, the gas volume during the contact period with the melt is assumed to be constant. Then the local mean pressure can be obtained by

$$P_1/T_1 = P_{\mathrm{m}}/T_{\mathrm{m}} \quad (4)$$

where P_1 is the initial pressure of the gas, and P_m the mean pressure of the gas at T_{m}. The temperature and the pressure versus the contact time are shown in Figs 5 and 6.

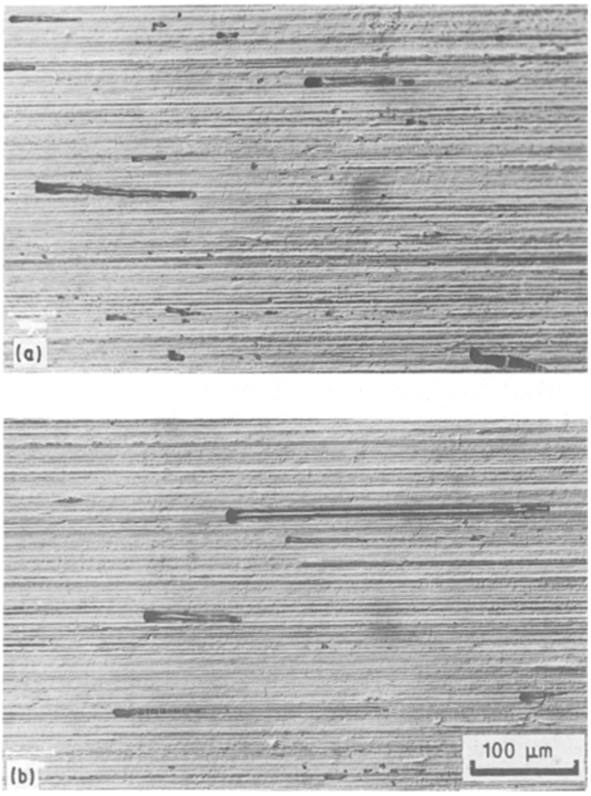

Figure 3 Contact patterns of the solidified ribbons, at a casting temperature of 353 K, and casting velocities of (a) 17.5 and (b) $20\ \mathrm{m\,s^{-1}}$.

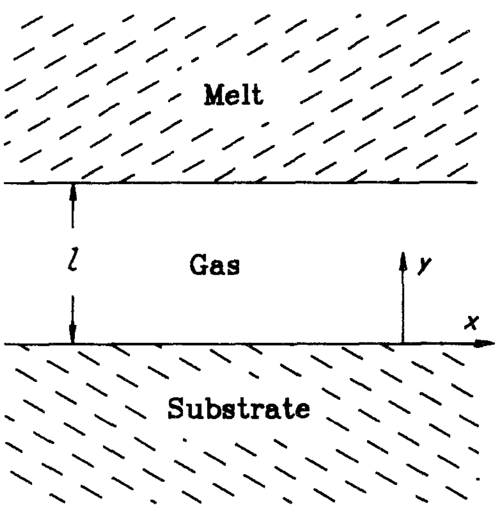

Figure 4 The entrapped gas between the melt and the substrate, the casting direction being into the paper.

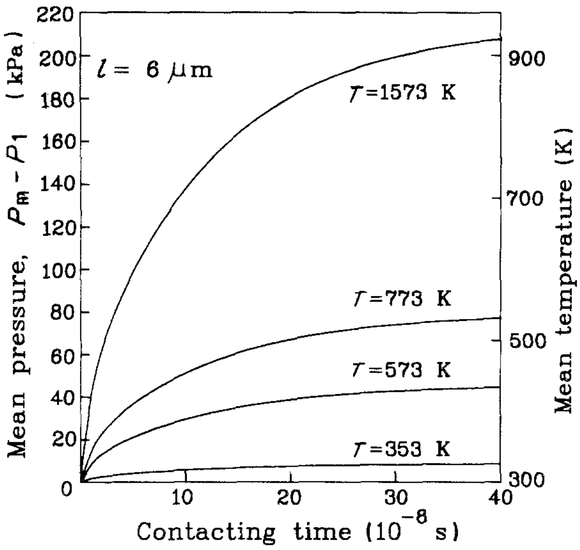

Figure 5 Pressure and temperature of the gas versus contact time with different casting temperatures.

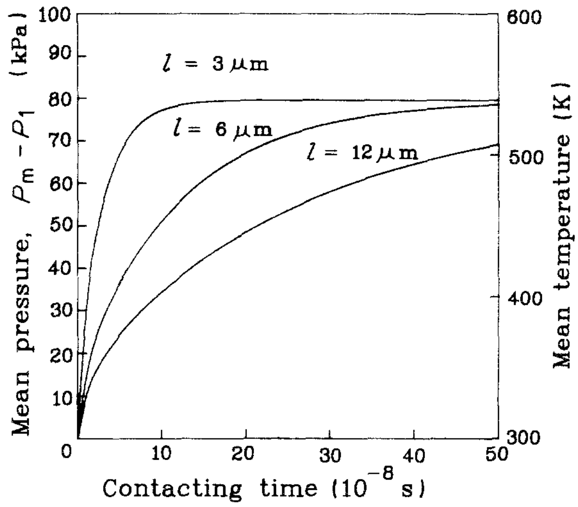

Figure 6 Pressure and temperature of the gas versus contact time at a casting temperature of 773 K and with different depths of the entrapped gas.

From Fig. 5, it is noted that the local pressure built up by the thermal effect is increased with increasing melt temperature, and it is far greater than the pressure of the gas-boundary layer. Even though the melt temperature is only 573 K, the local pressure of the entrapped gas built up by the thermal effect can increase by 45 kPa. Comparing this pressure with the dynamic pressure of the gas-boundary layer (about 0.24 kPa, at the casting velocity of $20\ \mathrm{m\,s^{-1}}$, in air [6]), it is manifest that the local pressure built up by the thermal effect is two orders higher, let alone the conventional liquid melt whose melt temperature is always higher than 1000 °C. As shown in Fig. 5, the local pressure of the entrapped gas developed by the melt at 1573 K, can even increase by 212 kPa. Thus, the higher the melt temperature, the more readily the air pocket is enlarged, as verified in the previous section.

The depth of the entrapped gas is only about several micrometres, thereby the rate of pressure build-up by the thermal effect is very fast, and is sensitive to the depth of the entrapped gas, as shown in Fig. 6 for the melt at 773 K. It is interesting to note that, even though the depth of the entrapped gas is 6 µm, the pressure is nearly fully developed during a contact time of 0.5 µs. At the casting velocity of $20\ \mathrm{m\,s^{-1}}$, 0.5 µs corresponds to a contact distance of 10 µm. The length of the air pockets in the casting direction is always greater than this value. The largest temperature difference between the melt and the gas is at the part of initial contact, i.e. the thermal effect is also most violent at this moment, suggesting that most of the thermal effect which enlarges the air pocket is developed near the open interface of the air pocket.

The above calculation results (local developed pressure) are based on the assumption of constant entrapped gas volume during the thermal effect. The real situation is a dynamic condition, in which the local pressure will contribute to enlarge the noncontact area, because it is impossible to increase the local pressure by several hundreds of kilopascals while keeping a constant volume of entrapped gas. The pressure built up to some extent will contribute to enlarge the volume of the entrapped gas. The enlarging area of entrapped gas near the open interface makes possible the incorporation of more gas from the gas-boundary layer into the liquid puddle (by the rotating substrate or pressure of the gas-boundary layer). As a result, the size of the air pocket is sensitive to the magnitude of the melt temperature.

The pressure of the gas-boundary layer impacts at the converging contact angle; at the same time, it also impacts at the free surface of the puddle and affects the puddle stability during casting. On the other hand, the thermal effect enhancing the gas entrapment only happens at the converging contact angle (or melt/substrate interface). Puddle stability is an important problem in the rapid solidification process. Many investigations have been concerned with increasing the puddle stability to decrease the size and amount of air pockets [11–19]. The size of the contact angle is anothor important consideration in gas entrapment [11] and is related to the puddle stability. If the converging contact angle is close to $\pi/2$, the thermal effect will not be possible. However, this condition does not seem likely to exist, as the melt on the wheel surface is rapidly dragged away by the substrate.

4. Conclusion

The pressure of the gas-boundary layer and the pressure induced by the thermal effect of the melt on the gas can both promote nucleation and growth of the air pockets during casting. From the heat-flow analysis, it is interesting to note that, due to the large temperature difference between the melt and the gas, the pressure built up by the thermal effect is greater than that by the gas-boundary layer effect. Owing to the small depth of the entrapped gas, the development of local pressure by the thermal effect is very fast (of the order of microseconds).

The experimental results show that the thermal effect of the melt on the gas can not only enlarge the air pockets, but also can facilitate air pocket formation. At higher casting velocities and extremely low casting temperatures, the air pocket formation is dominated by the gas-boundary layer effect (or poor puddle stability), and is characterized by the slender shape and the formation parallel to the casting direction. On the other hand, at higher casting temperatures, even though at low casting velocities, the air pocket is coarser in size than those induced by the gas-boundary layer effect only.

Acknowledgements

This research was sponsored by the National Science Council, Taiwan under contract no. NSC 77-0405-N009-04. The authors thank Professor J. D. Lin for valuable discussions.

References

1. M. C. NARASIMHAN, US Pat. 4 142 571 (1979).
2. H. FIEDLER, H. MUHLBACH and G. STEPANI, *J. Mater. Sci.* **19** (1984) 3229.
3. S. KAVESH, in "Metallic Glasses" edited by J. J. Gilmon and H. J. Leamy (ASM, Metals Park, OH, 1976) p. 36.
4. C. E. MOBLEY, R. E. MARINGER and L. DILLINGER, in "Rapid Solidification Processing" edited by R. Mehrabian, B. H. Kear and M. Coohen (Claitor's, 1978), p. 222.
5. S. C. HWANG and H. C. FIEDLER, *Met. Trans. A* **12** (1981) 1107.
6. P. CREMER and J. F. WADIER, in "Proceedings of 5th International Conference on Rapidly Quenched Metals V", Vol. 1, edited by S. Steeb and H. Warlimont (North-Holland, Amsterdam, 1985) p. 83.
7. F. E. LUBORSKY, S. C. HWANG and H. C. FIEDLER, *IEEE. Trans. Mag.* **17** (1981) 3463.
8. J. M. ROBERTSON, M. BROUHA, H. H. STEL and A. J. C. VAN DER BORST, in "Proceedings of 5th International Conference on Rapidly Quenched Metals V", Vol. 1, edited by S. Steeb and H. Warlimont (North-Holland, Amsterdam, 1985) p. 79.
9. T. TAKESHITA and P. H. SHINGU, *Trans. Jpn Inst. Metals* **27** (1986) 141.
10. R. S. TIMSIT, *Appl. Phys. Lett.* **40** (1982) 379.
11. S. C. HWANG, in "Proceedings of 4th International Conference on Rapidly Quenched Metals IV", Sendai, Japan, August 1981, Vol. 1, edited by T. Masumoto and K. Suzuki (Japan Institute of Metals, 1982) p. 65.
12. H. H. LIEBERMANN, *J. Mater. Sci.* **15** (1981) 2771.
13. D. PAVUNA, *J. Non-Cryst. Solids* **37** (1980) 133.
14. *Idem., J. Mater. Sci.* **16** (1981) 2419.
15. Y. SATO, T. SATO and Y. OKAZAKI, *Mater. Sci. Engng* **99** (1988) 73.
16. H. H. LEIBERMANN, in "Proceedings of 3rd International Conference on Rapidly Quenched Metals III", Vol. 1, edited by B. Cantor (Metals Society, London, 1978) p. 34.
17. M. MATSUURA, M. KIKUCHI, M. YAGI and K. SUZUKI, *Jpn J. Appl. Phys.* **19** (1980) 1781.
18. U. KOSTER, *Scripta Metall.* **17** (1983) 867.
19. RANJAN RAY, US Pat. 4 154 283 (1979).

Received 20 February 1990
and accepted 25 March 1991